

## Describing surfaces: Semi-infinite versus thin film approaches

P. Weinberger,<sup>1</sup> A. Vernes,<sup>2</sup> L. Szunyogh,<sup>3</sup> and J. Zablouil<sup>4</sup>

<sup>1</sup>*Center for Computational Nanoscience, Seilerstätte 10/22, A-1010 Vienna, Austria*

<sup>2</sup>*Austrian Center of Competence for Tribology, Viktor Kaplan-Straße 2, A-2700 Wiener Neustadt, Austria*

<sup>3</sup>*Department of Theoretical Physics, Budapest University of Technology and Economics, Budafoki út 8, H-1521 Budapest, Hungary*

<sup>4</sup>*Institute for Physical Chemistry, University of Vienna, Sensengasse 8/7, A-1090 Vienna, Austria*

(Received 3 April 2009; revised manuscript received 6 August 2009; published 27 August 2009)

In theoretical studies of the electronic structure and magnetic properties of solids with a surface thin film concepts as well as approaches based on semi-infinite geometries are used leading very often to quite similar results, but also sometimes substantial disagreement can be found in the literature. Furthermore, since usually different computational schemes are applied a direct comparison between the two basic concepts seems to be out of reach. By discussing the boundary conditions inherent to these two concepts and by making use of a model that combines on equal footing both aspects the main similarities but also differences can be pointed out. This model is applied to free and magnetically coated surfaces of fcc Cu(100) and fcc Pt(111) as well as to a free surface of bcc Fe(100). It is shown that local quantities such as surface spin and orbital moments can be determined equally well using either of the two concepts while the very details of the corresponding Friedel oscillations generally are much less compatible. In particular, for the magnetic anisotropy energy of magnetic overlayers on highly polarizable nonmagnetic substrates or of free surfaces of magnetic solids the conceptual differences become apparent.

DOI: [10.1103/PhysRevB.80.075430](https://doi.org/10.1103/PhysRevB.80.075430)

PACS number(s): 31.15.xr, 71.15.Ap, 75.70.Ak

### I. INTRODUCTION

In the last decade the study of surface-related properties became increasingly important. The arrival of high-resolution STM techniques and, in particular, the problem of perpendicular magnetism and giant magnetoresistance effects, virtually pushed also theoretical interests in the direction of solid systems with reduced dimensions. Since in the past studies of the electronic structure and magnetic properties of solids were entirely devoted to bulk materials which permitted one to use three-dimensional cyclic boundary conditions, new schemes and computational techniques had been developed in order to cope with less translationally periodic systems. Basically two quite different approaches based on two-dimensional translational invariance were introduced to describe solid systems with a surface, namely, one making use of the concept of thin films and the other one of semi-infinite geometries. The first one was a consequence of the use of wave-function methods (linearized augmented plane-wave or pseudopotential methods<sup>1</sup>), the second is mostly confined to Green's function techniques [Korringa-Kohn-Rostoker<sup>2</sup> (KKR) or linear muffin-tin orbital type approaches<sup>3</sup>]. Mainly because of different computational parameters and different aspects of convergence inherent to each method no rigorous comparison between the two underlying concepts has been made up to now. It is the aim of this communication to provide such a comparison by making use of one and the same numerical approach.

As is probably well-known evaluations of the electronic structure and magnetic properties of molecules or solid systems in terms of the density-functional theory (DFT) can be viewed as an iterative approach since a quantum mechanically derived differential equation is combined with an electrodynamic one, namely, the Poisson equation

$$H(\mathbf{r})\psi(\mathbf{r}, \epsilon_i) = \epsilon_i\psi(\mathbf{r}, \epsilon_i), \quad (1)$$

$$\Delta V(\mathbf{r}) = -8\pi\rho(\mathbf{r}), \quad (2)$$

$$\mathcal{N} = \int \rho(\mathbf{r})d^3r, \quad \rho(\mathbf{r}) = \sum_{-\infty < \epsilon_i \leq E_F} \psi^*(\mathbf{r}, \epsilon_i)\psi(\mathbf{r}, \epsilon_i). \quad (3)$$

In here  $H(\mathbf{r})$  is an appropriate Kohn-Sham Hamiltonian (nonrelativistic or relativistic),  $\rho(\mathbf{r})$  the (single-particle) density and  $E_F$  the Fermi energy (highest-occupied state in the case of molecules). Equally well known is the fact that the requirement of self-consistency of the Kohn-Sham equations (the very character of an iterative multiscale approach) implies to specify three boundary conditions: two for Eq. (1) to quantize the system, which clearly enough have to be in essence the same for the auxiliary classical differential Eq. (2), and one to fulfill the condition that the number of particles  $\mathcal{N}$  per characteristic volume in Eq. (3),<sup>4</sup> has to remain constant. Independent of the type of the exchange-correlation functional used in an actual calculation and of the method applied, these three boundary conditions have to be taken into account properly in any DFT calculation.

### II. SOLID SYSTEMS WITH A SURFACE

In principle, in a crystalline solid, characterized by three-dimensional translational invariance, the total volume  $\Omega$  can be written as

$$\Omega = \frac{N}{N_{at}}\Omega_0, \quad (4)$$

where  $N$  is the total number of atoms and  $\Omega_0$  is usually referred to as the volume of the unit cell or characteristic volume,  $N_{at}$  being the number of atoms per unit cell. Considering uniform two-dimensional translational invariance as is necessary to describe crystalline solids with a surface, the

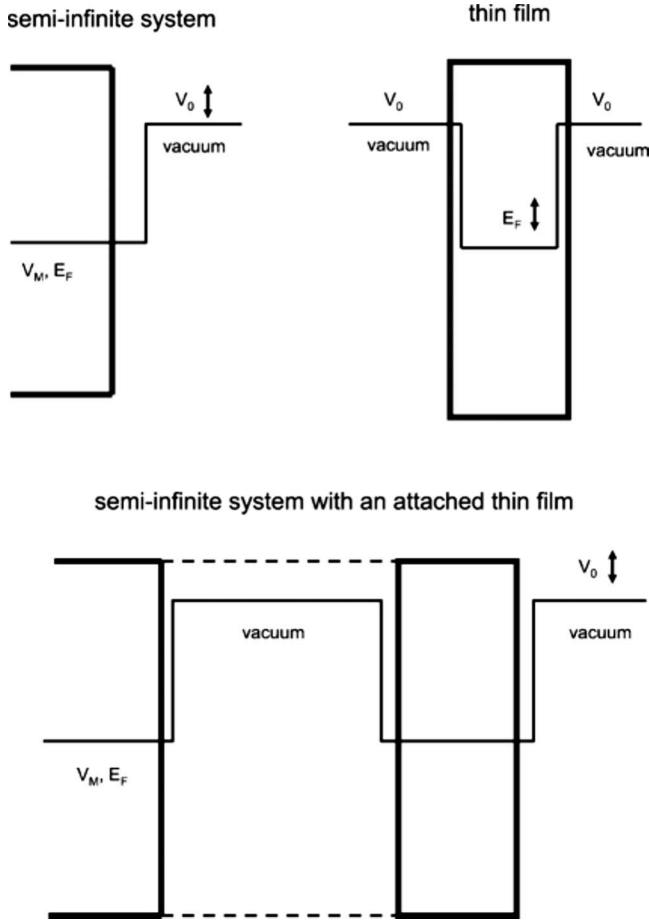


FIG. 1. Top: typical setup for a semi-infinite (left) and a thin film approach. Bottom: combining both aspect by attaching smoothly a thin film to a semi-infinite system.

characteristic volume  $\bar{\Omega}$  in a for matters of simplicity simple lattice (one atom per unit cell,  $N_{at}=1$ ) is defined by

$$\Omega = N_{\perp} N_{\parallel} \Omega_0, \quad (5)$$

$$\bar{\Omega} = \frac{\Omega}{N_{\parallel}} = N_{\perp} \Omega_0, \quad (6)$$

where  $N_{\perp}$  is the total number of atomic planes,  $N_{\parallel}$  is the order of the two-dimensional translational group, and  $\Omega_0$  the unit cell in the atomic planes.

In viewing  $\mathbf{r}$  in Eqs. (1)–(3) to consist of an in-plane component  $\mathbf{r}_{\parallel}$  and an orthogonal complement  $r_{\perp}$ ,

$$\mathbf{r} = (r_{\perp}, \mathbf{r}_{\parallel}), \quad (7)$$

and similarly translational vectors as

$$\mathbf{t} = (t_{\perp}, \mathbf{t}_{\parallel}), \quad \mathbf{t}_{\parallel} \in T, \quad (8)$$

$T$  being the (two-dimensional) translational group, then the boundary conditions for Eq. (1) can be formulated according to Fig. 1 as

$$\lim_{r_{\perp} \rightarrow +\infty} \psi(\mathbf{r}, \epsilon_i) = 0, \quad (9)$$

$$\lim_{r_{\perp} \rightarrow -\infty} \psi(\mathbf{r}, \epsilon_i) = \begin{cases} 0; & \text{thin film} \\ \psi(\mathbf{r} + \mathbf{t}_{\perp}, \epsilon_i); & \text{semi-infinite system} \end{cases} \quad (10)$$

which in turn implies for Eq. (2)

$$\lim_{r_{\perp} \rightarrow +\infty} V(\mathbf{r}) = V_0, \quad (11)$$

$$\lim_{r_{\perp} \rightarrow -\infty} V(\mathbf{r}) = \begin{cases} V_0; & \text{thin film} \\ V_M; & \text{semi-infinite system} \end{cases}, \quad (12)$$

where  $V_0$  is a constant<sup>5,6</sup> that characterizes the vacuum level and  $V_M$  is the so-called Madelung potential in a bulk system of the same material.<sup>2</sup> In Fig. 1 increasing values of  $r_{\perp}$  refer to the right-hand side of the individual figures while the corresponding left-hand side corresponds to decreasing values. Strictly speaking the boundary conditions in Eqs. (9) and (10) are only valid for a Kohn-Sham Hamiltonian with a discrete spectrum. In using Green's functions they easily can be extended to continuous states, see, e.g., Ref. 2.

These boundary conditions have consequences for achieving self-consistency, i.e., for conditioning the procedure to be performed. In the case of thin films the vacuum level  $V_0$  is fixed. Therefore, the only parameter that can be varied is the Fermi energy. For semi-infinite systems the Madelung potential  $V_M$  and the Fermi energy  $E_F$ , see Eq. (3), have to be kept fixed, meaning that the variational parameter can only be  $V_0$ .

Because of these different boundary conditions it is very often difficult to compare results obtained for semi-infinite systems with those using a thin film geometry. To combine both approaches and apply exactly the same numerical procedures, in here the model displayed in the lower part of Fig. 1 is applied. In this model a thin film is attached onto a semi-infinite system by means of a large enough vacuum barrier. Because in the center of this barrier  $\rho(\mathbf{r})$  is virtually zero, the spectra of the Kohn-Sham Hamiltonians characterizing the semi-infinite and the thin film part of the total system overlap only marginally. Therefore, two (nearly) individual systems are present, however, subject to the same boundary conditions:  $V_M$  and  $E_F$  are fixed and  $V_0$  is varied. Clearly, if the separating vacuum barrier to be determined self-consistently is thick enough, its value in the center is the same value as  $V_0$ .

### A. Semi-infinite systems

Once self-consistency has been reached Eq. (6) has to be recalled in order to evaluate physical properties, in particular, when trying to compare these with experimental data for a magnetically coated nonmagnetic substrate such as, for example, Cu(111)/Co. If, for example,  $d_{\text{exp}}$  is the experimental penetration depth (or escape length),

$$d_{\text{exp}} = d_{\perp} N_{\perp}, \quad (13)$$

where  $d_{\perp}$  is the interlayer distance and  $N_{\perp}$  corresponds now to an appropriate number of atomic planes, then, e.g., the averaged spin ( $\bar{m}_s$ ) and orbital ( $\bar{m}_o$ ) magnetic moments to be compared with experiment are given by

$$\bar{m}_s(N_\perp) = \frac{1}{N_\perp} \sum_{i=1}^{N_\perp} m_s^i, \quad \bar{m}_o(N_\perp) = \frac{1}{N_\perp} \sum_{i=1}^{N_\perp} m_o^i. \quad (14)$$

The anisotropy energy  $E_a$  referring in here to the energy difference between a uniform in-plane ( $\parallel$ ; along  $[100]$ ) and a uniform perpendicular ( $\perp$ ; along  $[001]$ ) to the planes of atoms orientation of the magnetization is usually defined<sup>2</sup> as the sum of two contributions, namely, the so-called band energy  $E_b$  (difference in corresponding grand potentials as determined by means of the magnetic force theorem<sup>7</sup>) and the magnetic dipole-dipole interaction  $E_{dd}$ ,  $E_a = E_b + E_{dd}$ . In viewing the anisotropy energy as a sum over layer-resolved contributions,

$$E_a = E_a(N_\perp) = \sum_{i=1}^{N_\perp} (E_b^i + E_{dd}^i), \quad (15)$$

$$E_b^i = \int [n_i(\perp; z) - n_i(\parallel; z)](E_F - z) dz, \quad (16)$$

$E_a$  has to be independent of the number of atomic layers considered, i.e.,

$$|E_a(N_\perp + k) - E_a(N_\perp)| \leq \delta, \quad (17)$$

and, therefore, also

$$|E_b(N_\perp + k) - E_b(N_\perp)| \leq \delta, \quad (18)$$

where  $k$  is an arbitrary positive integer and  $\delta$  an infinitesimal small number. In Eq. (16)  $n_i(C; z)$  is the density of states corresponding to the unit cell in the  $i$ th atomic layer and magnetic configuration  $C = \perp$  or  $\parallel$ . Equation (17) guarantees that the anisotropy energy is indeed a physical constant.<sup>8,9</sup>

For a nonmagnetic substrate coated with a few monolayers of a magnetic element, it is sufficient that  $N_\perp$  includes a rather small number of substrate layers in order to fulfill Eq. (17). Clearly, in the case of easily polarizable substrates such as Pd or Pt usually more substrate layers have to be self-consistently taken into account than for nonpolarizable substrates.

For a magnetic substrate, however, such as, for example, bcc Fe(100), Eqs. (13), (14), and (18) do have important consequences. If  $N_0$  denotes a large enough number (e.g.,  $N_0 = \sqrt[3]{N_L}$ ,  $N_L$  being the Avogadro number) then

$$\lim_{N_\perp \rightarrow N_0} \left[ \frac{E_b(N_\perp)}{N_\perp} \right] = E_b^{bulk}, \quad (19)$$

and consequently

$$\lim_{N_\perp \rightarrow N_0} \bar{m}_s(N_\perp) = m_s^{bulk}, \quad \lim_{N_\perp \rightarrow N_0} \bar{m}_o(N_\perp) = m_o^{bulk}. \quad (20)$$

Very clearly the reasons for being very careful with the summations in Eqs. (13), (14), and (18) are the famous Friedel oscillations, which by definition are of long-range character.

### B. Thin films

Because of computational restrictions in using a film geometry to describe surface-related properties the number of

atomic planes necessarily has to remain reasonably small. Thin films are characterized by two “surfaces” sandwiching a not too big number of substrate or carrier layers. Since now two Friedel oscillations in opposite directions exist, one can expect to observe a kind of standing-wave behavior instead of slowly dying off fluctuations. Furthermore, most of the equations from above have to be reformulated. If therefore because of computational restrictions  $N_\perp$  is reasonably small and denotes again the total number of atomic layers in a thin film (characterized by two-dimensional symmetry), then—because of enhancement effects at the surface—in the case of a thin film of a magnetic element such as, for example, bcc Fe(100), in principle,

$$\bar{m}_s^{film}(N_\perp) > m_s^{bulk}, \quad \bar{m}_o^{film}(N_\perp) > m_o^{bulk}, \quad (21)$$

and, in particular,

$$E_a^{film}(N_\perp) \approx \frac{1}{2} E_a(N_\perp), \quad E_b^{film}(N_\perp) \approx \frac{1}{2} \sum_{i=1}^{N_\perp} E_b^i. \quad (22)$$

For magnetically coated nonmagnetic metallic substrates  $E_b^{film}(N_\perp)$  obviously depends not only on the number of substrate layers in the interior (in particular, if a strongly polarizable substrate is present), but also, due to the superposition of two Friedel oscillations, whether this number is even or odd.

### III. COMPUTATIONAL DETAILS

All *ab initio* calculations were performed at the experimental lattice constant [bcc Fe(100): 5.27, fcc Cu(100): 6.8309, fcc Pt(111): 7.4137 a.u.] in terms of the spin-polarized (fully) relativistic screened KKR<sup>2</sup> method for a uniform direction of the magnetization pointing along the surface normal. In using the obtained self-consistent potentials and exchange fields the grand potentials, see Eqs. (15) and (16), were evaluated by means of a contour integration along a semicircle using a 16 points Gaussian-quadrature and 1830  $\vec{k}$  points per irreducible part of the surface Brillouin zone. It is utterly important to note that the analysis presented in the following is absolutely independent of relaxation effects, or, whether or not a full potential approach is applied. The only relevant requirement is that exactly the same numerical scheme is applied for two conceptually dif-

TABLE I. Systems investigated using exactly the same numerical procedures.

	System
1	fcc Cu(100)/Cu <sub>12</sub> /Vac <sub>6</sub>
2	fcc Cu(100)/Cu <sub>12</sub> /Co <sub>1</sub> /Vac <sub>5</sub>
3	fcc Cu(100)/Cu <sub>12</sub> /Co <sub>1</sub> /Vac <sub>12</sub> /Co <sub>1</sub> /Cu <sub>12</sub> /Co <sub>1</sub> /Vac <sub>6</sub>
4	fcc Pt(111)/Pt <sub>12</sub> /Co <sub>1</sub> /Vac <sub>5</sub>
5	fcc Pt(111)/Pt <sub>12</sub> /Co <sub>1</sub> /Vac <sub>10</sub> /Co <sub>1</sub> /Pt <sub>12</sub> /Co <sub>1</sub> /Vac <sub>5</sub>
6	bcc Fe(100)/Fe <sub>n</sub> /Vac <sub>6</sub>
7	bcc Fe(100)/Fe <sub>n</sub> /Vac <sub>12</sub> /Fe <sub>n</sub> /Vac <sub>6</sub>

TABLE II. WF, vacuum level in the center of the combined system ( $V_{center}$ ), vacuum level ( $V_0$ ) outside the total system, and total band-energy contribution to the anisotropy energy for the Cu- and Pt-related systems.

System	WF (eV)	$V_{center}$ (ryd)	$V_0$ (ryd)	$E_b$ (meV)	$E_b/surface$ (meV)
1	5.312		0.2960		
2	5.619		0.31863	-0.433	-0.433
3	5.631	0.31928	0.31948	-1.309	-0.436
4	5.454		0.36241	0.091	0.091
5	5.465	0.36307	0.36321	0.532	0.177

ferent types of boundary conditions. The discussion excludes explicitly supercell approaches, since per definition when using three-dimensional cyclic boundary conditions there is no surface.

#### IV. RESULTS AND DISCUSSIONS

In Table I the systems investigated are listed. As can be seen from this table three typical kinds of systems were considered, namely, bcc Fe(100) and fcc Cu(100) as examples for magnetic and nonmagnetic solid systems with a surface as well fcc-Cu(100) and fcc-Pt(111) coated with one monolayer (ML) of Co. In the case of semi-infinite systems with an attached thin film, the separating vacuum barrier corresponds to a distance of 16.73 a.u. for Fe, 21.67 a.u. for the Cu-related system, and 22.65 a.u. in the case of the Pt system, i.e., in turn to 0.885, 1.147, and 1.199 nm. It turned out that the remaining charge in the center layers of the vacuum barrier was less than  $10^{-8}$  per unit cell. The notation used in this table gives account of the type and orientation of the substrate, the number of atomic layers on top and the number of empty (vacuum) layers that were included in the self-consistent calculations. It should be noted that in all figures the indexing of atomic layers refers to this notation; layer indices of less than one denote (uniform) bulk layers, see also, in particular, the lower part of Fig. 1.

In Tables II and IV the main characteristics of these systems such as the work function (WF), the value of the

TABLE III. Spin and orbital moments and the layer-resolved contributions of the Co layer in the Cu- and Pt-related systems.

System	Surface layer	$m_s$ ( $\mu_B$ )	$m_0$ ( $\mu_B$ )	$E_b^i$ (meV)
2	1	1.8351	0.1426	-0.390
3	1	1.8351	0.1426	-0.390
	2	1.8302	0.1427	-0.393
	3	1.8302	0.1427	-0.393
4	1	2.0038	0.1504	0.184
5	1	2.0038	0.1504	0.184
	2	2.0037	0.1510	0.220
	3	2.0037	0.1510	0.220

TABLE IV. WF, vacuum level in the center of the combined system, vacuum level outside the total system, and total band-energy contribution to the anisotropy energy for Fe-related systems.

System	$n$	WF (eV)	$V_{center}$ (ryd)	$V_0$ (ryd)	$E_b$ (meV)	$E_b/surface$ (meV)
6	12	5.004		0.36592	0.283	0.283
	15	5.004		0.36592	0.285	0.285
	18	5.004		0.36588	0.290	0.290
7	12	4.982	0.36488	0.36432	0.861	0.287
	18	5.009	0.36602	0.36629	0.775	0.258

vacuum level in the center of the separating vacuum barrier ( $V_{center}$ ) and the vacuum barrier (right boundary condition,  $V_0$ ) are displayed together with the band energy contribution to the anisotropy energy. Tables III and V deal with the actual surface layers. In there the spin and orbital moment as well as the contribution of the surface layer to the band energy are listed. In these tables the entry “surface layer” numbers (from the left to right) subsequent surfaces as depicted in the lower part of Fig. 1.

As easily can be seen from these tables, for the Cu-related systems the differences between the results for a thin film and the ones for the corresponding semi-infinite system seem to be minute. Even in the case when a Co overlayer forms the surface corresponding layer-resolved band energies are virtually the same. In the case of the Fe-related systems the differences are slightly bigger. In particular, a small variation with respect to the thickness in the spin moment can be read off, although still only on the order of less than about  $0.01 \mu_B$ .

In order to trace the differences between the two theoretical concepts the very details of the Friedel oscillations, in particular, well inside the film or the semi-infinite systems, have to be investigated. To show these oscillations in the case of the Cu-related systems, in Fig. 2 the layer-resolved spin and orbital moments and band energies are displayed for the system fcc Cu(100)/Cu<sub>12</sub>/Co<sub>1</sub>/Vac<sub>12</sub>/Co<sub>1</sub>/Cu<sub>12</sub>/Co<sub>1</sub>/Vac<sub>6</sub>. In these figures the respective top parts refer to the global views by showing the contributions from all layers. In the lower

TABLE V. Spin and orbital moments and the layer-resolved contributions of the surface layer in the Fe-related systems.

System	$n$	Surface layer	$m_s$ ( $\mu_B$ )	$m_0$ ( $\mu_B$ )	$E_b^i$ (meV)
6	12	1	2.8679	0.0919	0.293
	15	1	2.8673	0.0916	0.291
	18	1	2.8670	0.0916	0.292
7	12	1	2.8679	0.0919	0.293
		2	2.8655	0.0908	0.293
	18	3	2.8655	0.0908	0.293
		1	2.8684	0.0918	0.296
		2	2.8796	0.0908	0.280
		3	2.8796	0.0908	0.280

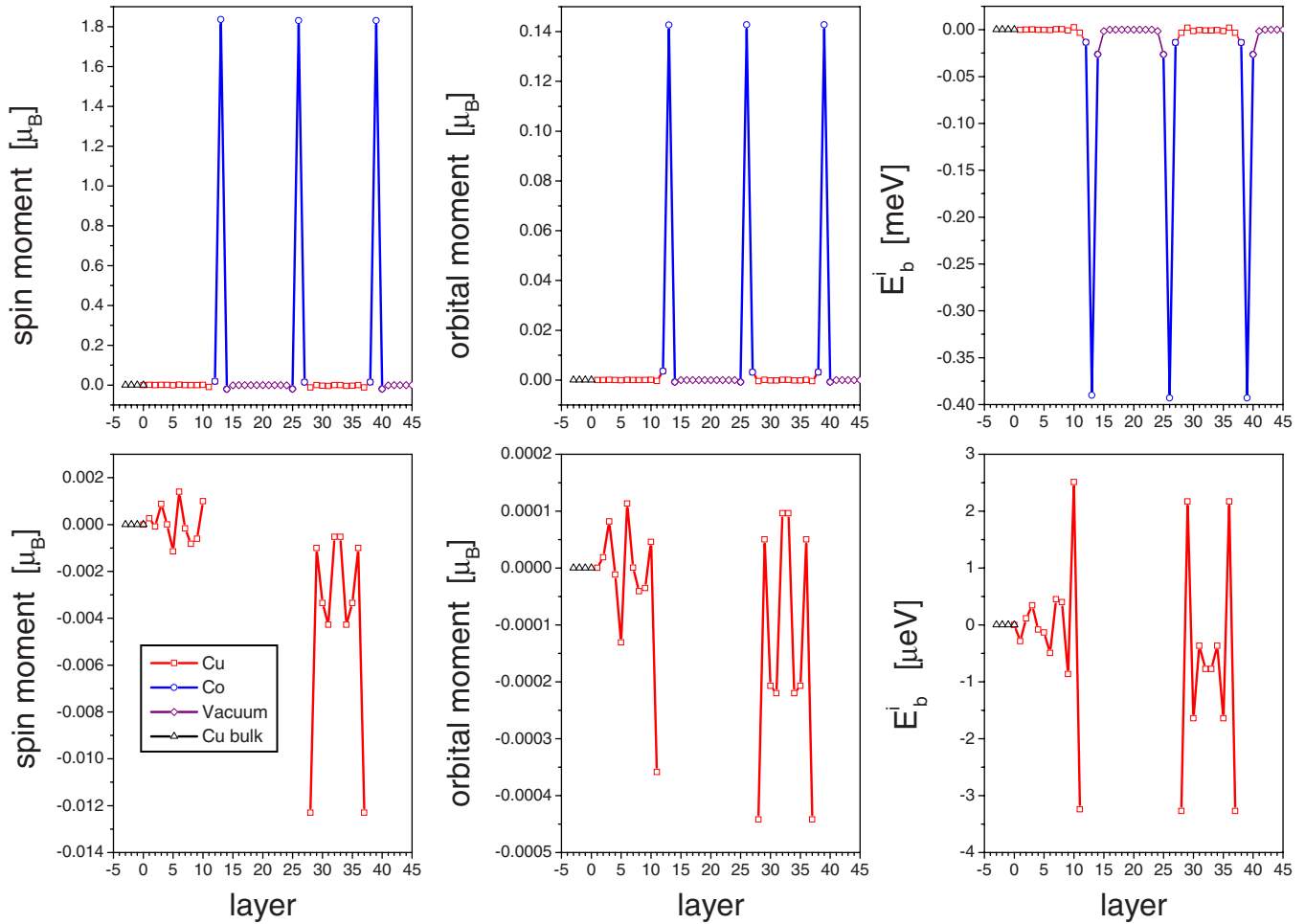


FIG. 2. (Color online) fcc Cu(100)/Cu<sub>12</sub>/Co<sub>1</sub>/Vac<sub>12</sub>/Co<sub>1</sub>/Cu<sub>12</sub>/Co<sub>1</sub>/Vac<sub>6</sub>. Top: layer-resolved spin moments (left), orbital moments (middle), and band-energy contributions to the anisotropy energy (right) through out the whole system. Bottom: excluding the surface layer and the first one below.

parts the contributions from the surface layer and the layer below are excluded. In Fig. 3 the same quantities are displayed for the Pt-related systems. As can be seen from these figures, globally, i.e., for the surface layer and the layer beneath both the semi-infinite case as well as a thin film lead to virtually the same results. See in particular the upper halves of Figs. 2 and 3 and Tables II and III. In the interior of the Cu or Pt substrate, however, significant differences between a semi-infinite and a thin film geometry are noticeable, which of course are caused by the different boundary conditions (see the lower parts of these figures). In the case of the semi-infinite systems for Cu as well as for Pt the spin and orbital moments converge to zero in about 6–8 atomic layers below the magnetic surface. Quite obviously the oscillations of the orbital moments in a Cu or Pt film are significantly bigger than in a semi-infinite substrate. In particular, interesting is to compare the band energy entries in Fig. 2 with those in Fig. 3. First of all, contrary to the Cu system in the Pt system the contribution from the second layer below the surface (−0.16 meV) is in size almost as big as the contribution from the Co layer (0.18 meV). Since these two contributions are of opposite sign the value of the total band energy is rather small. Second, because of this effect the layer-resolved

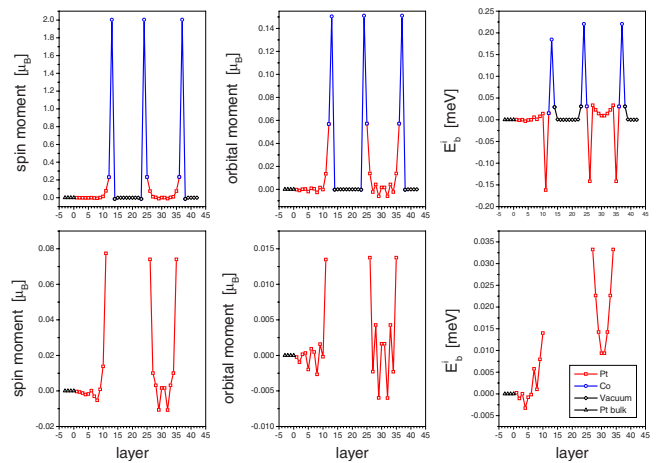


FIG. 3. (Color online) fcc Pt(111)/Pt<sub>12</sub>/Co<sub>1</sub>/Vac<sub>10</sub>/Co<sub>1</sub>/Pt<sub>12</sub>/Co<sub>1</sub>/Vac<sub>5</sub>. Left: layer-resolved spin moments (left), orbital moments (middle), and band-energy contributions to the anisotropy energy (right) through out the whole system. Bottom: excluding the surface layer and the first two below. In the case of the band energies the surface layer and the first two below are excluded.

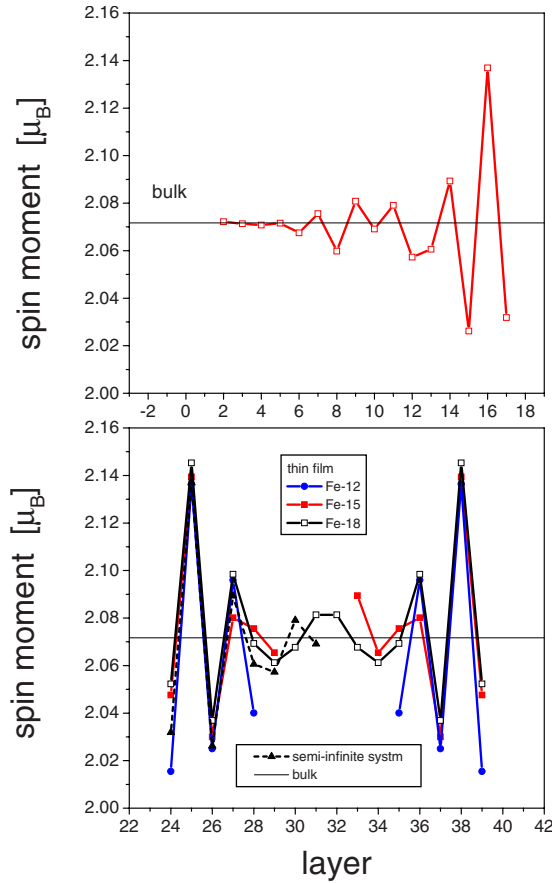


FIG. 4. (Color online) Top: oscillation of the spin moment from the surface to the bulk in the case of a semi-infinite bcc-Fe(100) system. Bottom: oscillation of the spin moment in a thin bcc-Fe film for different thicknesses. For comparison also a corresponding curve for a semi-infinite system is shown. In both figures the entries for the respective surface layer are excluded. Note that due to plotting purposes for  $Fe_n$ ,  $n < 18$ , the corresponding data are shown with respect to the layer indexing for  $n = 18$ .

band energy in the interior of the film or the semi-infinite substrate are in size considerably bigger than in the Cu system. This comparison not only shows very clearly the difference between a polarizable and a nonpolarizable substrate but also the significance of the different boundary conditions discussed in Eqs. (9)–(12). Furthermore, by inspecting the entries  $E_b^i$ /surface in Table II for the Pt-related systems, it is immediately apparent that as a consequence of the different boundary conditions there is almost a factor of 2 between the two corresponding values!

The top part of Fig. 4 serves as a nice example for the long-range character of the Friedel oscillations: only about 15 layers below the surface the bulk value of Fe is reached, which as can be seen from Table V is substantially smaller than that in the surface layer. The lower part of Fig. 4, in which the variation in the spin moments in the interior of Fe films of different thickness is displayed, proves that for the shape of the oscillations it is important whether the number of layers in the film is even or odd. Furthermore, as can be seen from Fig. 5, for an Fe film the surface magnetic moment does vary with the film thickness, while in the case of a

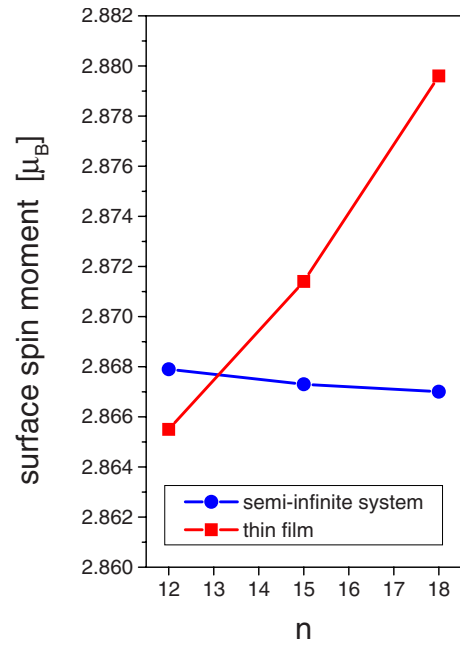


FIG. 5. (Color online) Variation in the spin moment of the surface layer with respect to the thickness of the surface-near region in bcc Fe(00) and a thin film of bcc Fe(100). See also Table I.

semi-infinite geometry it is nearly constant for a thickness beyond 12 ML.

Finally, in Fig. 6 the variation in the layer-resolved band energy, see Eqs. (15) and (16), is depicted for 12 and 18 MLs. In order to interpret this figure properly one has to recall Eqs. (19) and (22), and view again Fig. 1. Since as stated in Eq. (19), in the semi-infinite case  $E_b^i$  has to approach its bulk value, namely, zero, by increasing the number of Fe layers beneath the surface layer,  $E_b^i$  will oscillate only very slowly around this value. The contributions from

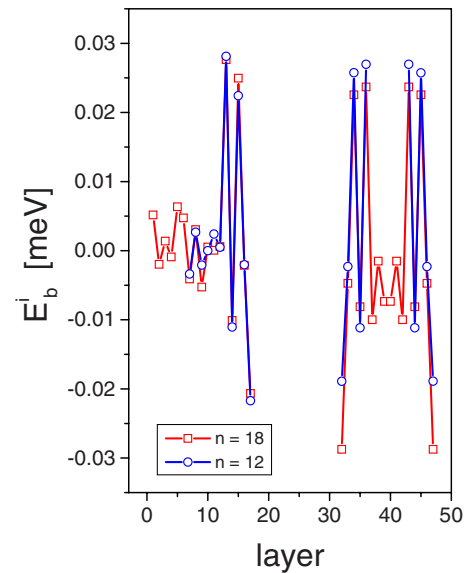


FIG. 6. (Color online) Variation in the layer-resolved band energies excluding the corresponding surface layers in bcc Fe(100)/ $Fe_n$ /Vac<sub>12</sub>/Fe<sub>n</sub>/Vac<sub>6</sub>.

surface-near layers (the surface layer and two layers below), however, seem to be independent from the number of further substrate layers. This also applies to the thin film case, which in turn implies there that the band-energy contribution to the anisotropy energy is mostly determined by these layers. As easily can be seen the oscillation in  $E_b^i$  is quite different from that in the semi-infinite case and depends on the thickness of the film.

## V. CONCLUSIONS

The above shown tables and figures indicate that—apart from differences in the Friedel oscillations—thin film geometries can indeed be used to describe global physical quantities of nonmagnetic metallic substrates with magnetic adlayers such as spin moments and orbital moments quite accurately, provided that the films are thick enough. Quite likely, they are not suitable to track Friedel oscillations correctly. For example, in order to reproduce the Friedel-type oscillations in the top part of Fig. 6 in a film (at least) a thickness of 36 layers would be necessary. In the case of free surfaces of a magnetic metal results for the magnetic properties when using a thin film approach are at least conceptually questionable, see Eqs. (21) and (22), while other properties such as the work function most likely will turn out to be in excellent agreement with their semi-infinite counterparts.

In the present calculations the Fermi energy, because of the special model used, was always that of the (semi-infinite) bulk. In thin film approaches the variational parameter is the Fermi energy and therefore at each thickness another Fermi energy applies. In order to make this point very clear: con-

sider fcc Cu(100) as a substrate covered with an increasing number of Co layers. The system to be investigated is then of the type  $\text{Co}_n/\text{Cu}_m/\text{Co}_n$ . If  $E_F(m, n)$  denotes the Fermi energy for a particular choice of  $n$  and  $m$  then in the extreme case that  $n \gg m$  not Cu coated with Co is described but a kind of spin valve with Co leads and Cu as a spacer.

Used with care and being aware of the boundary conditions inherent to the underlying scheme, (full potential) thin film approaches can offer substantial advantages. In the last by now almost 20 years they contributed a lot to the computational materials science of solid systems with surfaces, in particular, in the context of surface relaxations. Regrettably, up to now, none of the thin film approaches makes use of the Dirac equation, a fact that per se can cause differences in describing magnetic anisotropies. Thin film methods are perhaps less useful when, for example, trying to evaluate optical or magneto-optical properties, since the elements the layer-resolved permittivity tensor necessary, e.g., to evaluate Kerr angles including all interferences and reflections, become constant only deep inside the bulk. On the other hand, full potential semi-infinite approaches, although working even on a fully relativistic level, are presently still much too expensive to be used as standard methods of choice for matters of structure optimization. Both concepts, thin films or semi-infinite systems, offer different computational advantages, are very suitable for particular purposes and less suitable for others, all aspects being of course a matter of awareness of the underlying boundary conditions.

## ACKNOWLEDGMENT

One of the authors (L.S.) acknowledges support provided by the Hungarian National Scientific Research Fund (Contracts No. OTKA K68312 and No. K77771).

<sup>1</sup>D. J. Singh and L. Nordström, *Plane Waves, Pseudopotentials and the LAPW Method* (Springer, Berlin, New York, 2006).

<sup>2</sup>J. Zabloudil, R. Hammerling, L. Szunyogh, and P. Weinberger, *Electron Scattering in Solid Matter* (Springer, Berlin, New York, 2004).

<sup>3</sup>I. Turek, V. Drchal, J. Kudrnovský, M. Šob, and P. Weinberger, *Electronic Structure of Disordered Alloys, Surfaces and Interfaces* (Kluwer, Boston/London/Dordrecht, 1997).

<sup>4</sup>This equation can of course be written also in terms of Green's functions, see, e.g., Ref. 2.

<sup>5</sup>M. Weinert, *J. Math. Phys.* **22**, 2433 (1981); G. H. Schadler, *Phys. Rev. B* **45**, 11314 (1992).

<sup>6</sup>For a formal discussion of the Poisson equation for two- and three-dimensional translationally invariant systems see

chapter 20 of Ref. 2.

<sup>7</sup>H. J. F. Jansen, *Phys. Rev. B* **59**, 4699 (1999).

<sup>8</sup>It should be noted that different physical properties can require different characteristic volumina. This applies in particular when evaluating electric or magneto-optical properties.

<sup>9</sup>I. Reichl, A. Vernes, C. Sommers, L. Szunyogh, and P. Weinberger, *Philos. Mag.* **84**, 2543 (2004); A. Vernes, I. Reichl, P. Weinberger, L. Szunyogh, and C. Sommers, *Phys. Rev. B* **70**, 195407 (2004); I. Reichl, A. Vernes, P. Weinberger, L. Szunyogh, and C. Sommers, *ibid.* **71**, 214416 (2005); For a detailed discussion, see also P. Weinberger, *Magnetic Anisotropies in Nanostructured Matter* (CRC Press, Boca Raton/London/New York, 2008), Chap. 18.